Pergamon

Tetrahedron Letters 42 (2001) 4187–4190

TETRAHEDRON LETTERS

Carbon-centered dendritic radicals: photoinduced reaction of poly(benzyl ether) dendrons σ-bonded to a rhodium(III) porphyrin focal core

Shu-ichi Kimata and Takuzo Aida*

Department of Chemistry and Biotechnology, Graduate School of Engineering, The University of Tokyo, 7-3-1 Hongo, Bunkyo-ku, Tokyo 113-8656, Japan

Received 12 March 2001; revised 23 April 2001; accepted 27 April 2001

Abstract—Poly(benzyl ether) dendrons σ-bonded by the focal dialkoxybenzyl unit to a rhodium(III) porphyrin functionality (**1**-L*n*, $n=1$, 3–5) were synthesized as novel carbon-centered free radical equivalents. Upon excitation with visible light in a carbon monoxide atmosphere, **1**-L*n* ($n=1$, 3–5) underwent homolysis at the alkyl–rhodium bond to give the corresponding acylrhodium species **2**-L*n* ($n=1$, 3–5), where the consumption rate of **1**-L*n* was dependent on the generation number of the dendron unit. In particular, **1**-L5 bearing the largest dendron unit was much reluctant to undergo photochemical reactions.

Tuning of the reactivity of free radicals is an important subject in organic and macromolecular syntheses.[1] From this point of view, dendrimers, tree-like hyperbranched macromolecules with predictable three-dimensional shapes, are interesting as sterically encumbered media for generating 'constrained radicals'. Dendritic macromolecules generally consist of a focal core, many building blocks, and a number of exterior termini, where certain functionalities can be incorporated site-specifically into their three-dimensional archi-

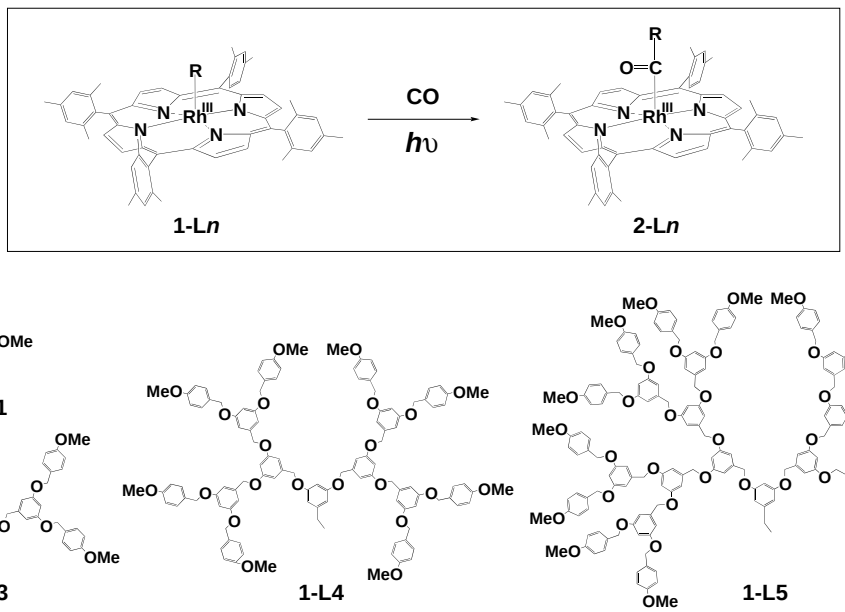

Scheme 1.

* Corresponding author.

0040-4039/01/$ - see front matter
PII: S0040-4039(01)00685-2

tectures. So far, there have been reported several examples of the incorporation of stable organic radicals into dendritic branches,[2] as pendant groups on the exterior surface,[3] and as non-covalently bound encapsulated guests in the interior void.[4] On the other hand, poly(benzyl ether) dendrons having a nitroxy radical at the focal core has been used for free radical polymerization of vinyl monomers,[5] where the active end of the polymer chain, in the form of a nitroxide adduct, is temporarily dissociated from the dendrimer scaffold, and the resulting free radical undergoes chain growth. Although reactivities of free radicals in dendrimer matrices are thus interesting, no examples of 'carbon-centered dendritic free radicals' have been reported so far.

We herein report synthesis and photoinduced reaction of poly(benzyl ether) dendrons σ-bonded by the focal dialkoxybenzyl core to the axial position of a rhodium(III) porphyrin (**1**-L*n*, $n=1$, 3–5). Since carbon–rhodium bonds in organorhodium(III) porphyrins can be cleaved homolytically by visible light,[6] **1**-L*n* are regarded as carbon-centered free radical equivalents. Thus, the dendritic rhodium complexes should allow exploration of possible effects of dendrimer matrices on reactivities of carbon-centered free radicals at the focal point. We investigated photoinduced reaction of **1**-L*n* ($n=1$, 3–5) with carbon monoxide (CO) to form acylrhodium species (**2**-L*n*) (Scheme 1). It should also be considered that poly(benzyl ether) dendrimers bear many 'chain-transferable' benzyl units, which may react with the focal point free radical in competition with carbon monoxide. In the present communication, we wish to highlight a clear 'dendrimer effect' on the reaction profile of the highest-generation **1**-L5.

1-L*n* ($n=1$, 3–5) were synthesized according to a procedure reported for the preparation of alkylrhodium(III) porphyrin complexes.[7] Thus nucleophilic rhodium(I) porphyrins, generated upon reduction of iodorhodium(III) tetramesitylporphyrin (TMP)RhI with $NaBH_4$, were allowed to react with 3,5-dimethoxylbenzyl bromide or poly(benzyl ether) dendritic bromides (L*n*Br, $n=3$–5)[8] to give **1**-L*n* ($n=1$, 3–5), which were identified by UV–vis and ^{1}H NMR spectroscopies together with mass spectrometry.[9] **1**-L3 and **1**-L4 were obtained in 67 and 61% yield, respectively, while the highest-generation **1**-L5 was obtained in only 19% yield probably due to a steric reason.

A typical example of the photoinduced reaction of **1**-L*n* under CO was given below: CO was bubbled for 10 min at a flow rate of 3.0 mL min^{-1} through a thin needle into a 1.0 μM C_6D_6 solution (0.8 mL) of **1**-L5 at 10°C in a NMR tube, which was then sealed off. The resulting CO-saturated solution was irradiated at 10°C with a xenon arc light (λ >445 nm) from a distance of 15 cm. In the ^{1}H NMR spectrum, a doublet signal due to $ArCH_2$ directly attached to Rh^{III} (δ −3.05 ppm) and a singlet signal due to pyrrole-β protons of the porphyrin ring (δ 8.72 ppm) gradually disappeared with irradiation time, while new signals at δ −1.50 ($ArCH_2(CO)Rh^{III}$) and δ 8.80 (pyrrole-β) ppm, assignable to those of the corresponding acylrhodium species (**2**-L5), appeared and grew (Fig. 1). Infrared spectroscopy of the reaction mixture showed a strong C=O vibrational band at 1720 cm^{-1} due to $ArCH_2(CO)Rh^{III}$.[10]

The rate of consumption of **1**-L*n*, as evaluated from the intensity of the ^{1}H NMR signal due to pyrrole-β protons of **1**-L*n*, relative to that of *p*-Me in the *meso*-aryl groups of (TMP)Rh, was found to depend remarkably on the generation number of the dendron unit (●, Fig. 2). For example, **1**-L1 (L1 = 3,5-dimethoxybenzyl), a non-dendritic reference, under irradiation was rapidly consumed in only 40 s. On the other hand, the consumption of dendritic **1**-L3 and **1**-L4, under identical conditions to the above, was definitely slower than that of **1**-L1. Although the rates of consumption of these two dendritic complexes appear not much different from each other, the highest-generation **1**-L5 was consumed more sluggishly than these lower generation homologues. On the other hand, as for the carbonylation of **1**-L*n* (○, Fig. 2), non-dendritic **1**-L1 was rapidly and selectively converted into **2**-L1. In contrast, the formation of acylrhodium species **2**-L*n* from dendritic **1**-L*n* ($n=3$–5) was much slower, regardless of the generation number of the dendron unit. Furthermore, the apparent selectivity of the carbonylation was also lower, indicating the occurrence of competitive side reactions inherent to the poly(benzyl ether) dendritic structure.

Upon photoexcitation under CO, dendritic **1**-L*n* undergoes homolysis at the carbon–rhodium(III) bond to give temporarily a rhodium(II) porphyrin metalloradical ($(TMP)Rh^{II}$) and a dendron with a carbon-centered free radical at the focal point (L*n*$^\bullet$), which then reacts with CO to give **2**-L*n* or recombines with $(TMP)Rh^{II}$ to revert to **1**-L*n* (Fig. 3). In addition to these reactions, L*n*$^\bullet$ can also undergo some side reactions such as hydrogen abstraction from CH_2 in the dendron unit or

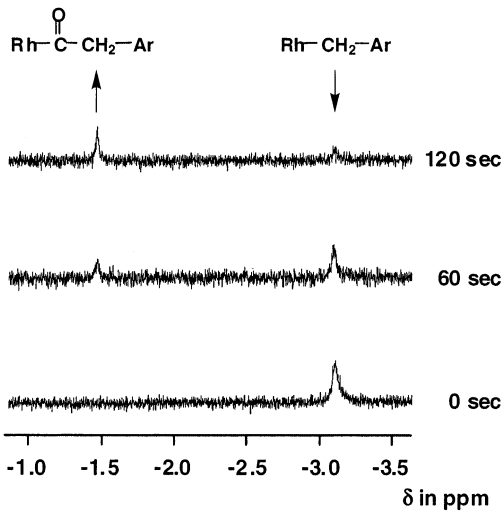

Figure 1. ^{1}H NMR spectral change profile at an upfield region upon photoexcitation of **1**-L5 in a carbon monoxide atmosphere in C_6D_6 at 10°C.

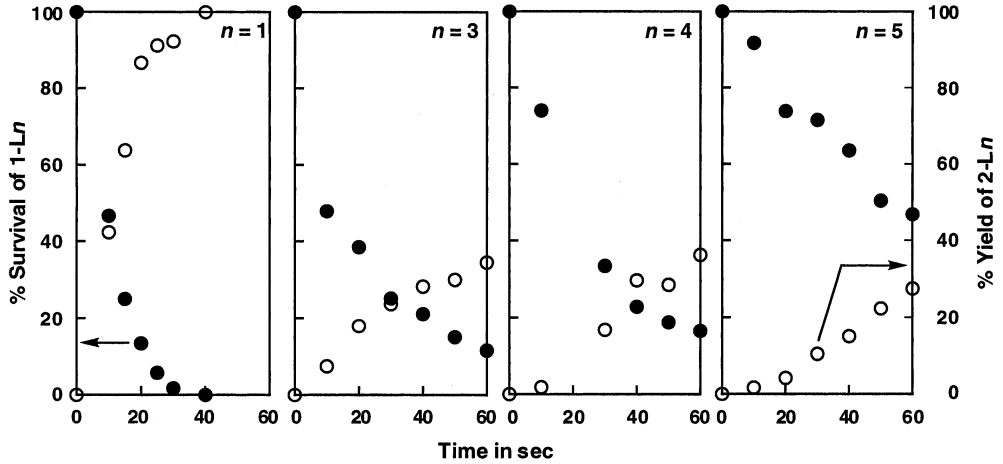

Figure 2. Irradiation of **1**-L*n* ($n=1$, 3–5) in C_6D_6 at 10°C with visible light (λ >445 nm) in a carbon monoxide (CO) atmosphere. Time courses of percentage survival of **1**-L*n* (●) and percentage yield of acylrhodium species **2**-L*n* (○), as evaluated from the intensity of the ^{1}H NMR signal due to pyrrole-β protons of **1**-L*n* and **2**-L*n*, relative to that of *p*-Me in the *meso*-aryl groups of the rhodium porphyrin, respectively.

recombination with L*n*$^\bullet$ to give L*n*–L*n*. Considering a low concentration of **1**-L*n* (1 μM) under the reaction conditions, such a hydrogen abstraction, if any, most likely occurs in an intramolecular fashion. Also in relation to this, no MALDI-TOF-MS peak due to L*n*–L*n* was detected irrespective of the generation number of L*n*. At any rate, the overall reaction profiles in Fig. 2 should reflect a possible competition of all the elementary reactions in Fig. 3. In the case of the highest-generation **1**-L5, a large hydrodynamic volume of the photodissociated dendron (L5$^\bullet$) would not allow a rapid diffusion of the focal free radical core from (TMP)Rh^{II}, so that the recombination of these paired radicals is very easy to occur. This can account for the apparently low susceptibility of **1**-L5 toward photolysis (Fig. 2). The same may hold true for **2**-L5 under irradiation. In relation to this trend, **1**-L5 in an argon atmosphere without CO also showed a very low susceptibility to photodecomposition, where the absorption spectral change, e.g. at 413.5 nm, characteristic of organorhodium(III) porphyrins, occurred much more slowly than that of **1**-L1. In Fig. 2 (●), lower-generation **1**-L3 and **1**-L4 appear to show an intermediate susceptibility inbetween those of **1**-L5 and non-dendritic **1**-L1. On the other hand, as for the apparent carbonylation rate of **1**-L*n* (○, Fig. 2), no substantial difference among the three dendritic compounds suggests only a little effect of the generation number of the dendron unit on the local steric environment around the reaction site. A CPK model study showed a rather open architecture around the carbon–rhodium bond even in the highest-generation **1**-L5, since the dendron unit can adopt a conical shape. It is likely that the transition state for the carbonylation of L5$^\bullet$ is similar to that for the recombination of L5$^\bullet$ to (TMP)Rh^{II}, since neither of them requires any conformational change around the focal core. Thus, the relative rate of these two reactions should depend on the diffusibility of the focal free radical core from (TMP)Rh^{II}. On the other hand, side reactions involving benzylic CH_2 requires some conformational change of the dendron unit, which must be relatively slow in the largest L5$^\bullet$. As a consequence of these situations, the carbonylation of **1**-L5 takes place with the highest selectivity among the family of dendritic **1**-L*n* ($n=3$–5).

In summary, through studies on photoinduced reactions of a series of rhodium(III) porphyrins having σ-bonded dendritic axial ligands with different generation numbers (**1**-L*n*, $n=1$, 3–5) under carbon monoxide, a clear threshold was observed for the effect of the generation number on the reactivity of a carbon-centered free radical at the focal point of the dendron unit. The unique reactivity of the highest-generation **1**-L5 is most likely due to a slow diffusibility and a low conformational change activity of the resulting dendritic radical (L5$^\bullet$). The present observation suggests a new guideline principle for the control of free radical-mediated organic transformations by dendritic architectures.

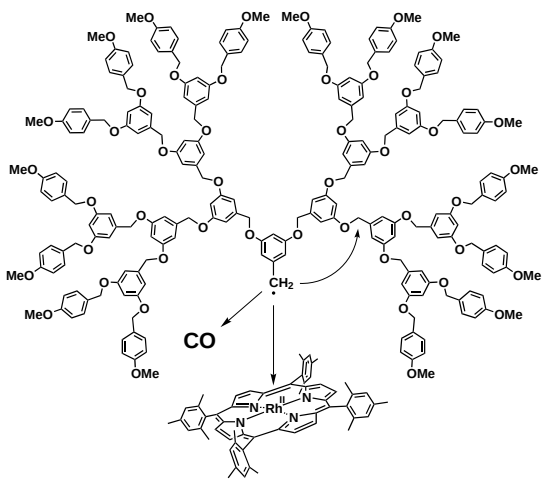

Figure 3. Schematic representation of possible reaction loci of a photodissociated dendritic radical.

References

1. (a) Renaud, P.; Gerster, M. *Angew. Chem., Int. Ed.* **1998**, *37*, 2562–2579; (b) Sibi, M. P.; Poter, N. A. *Acc. Chem. Res.* **1999**, *32*, 163–171; (c) Sawamoto, M.; Kamigaito, M. *J. Macromol. Sci. Pure. Appl. Chem.* **1997**, A (34), 1803–1814; (d) Hawker, C. J. *Acc. Chem. Res.* **1997**, *30*, 373–382; (e) Matyjaszewski, K. *Chem. Eur. J.* **1999**, *5*, 3095–3102.
2. (a) Rajca, A.; Utamapanya, S. *J. Am. Chem. Soc.* **1993**, *115*, 10688–10693; (b) Matsuda, K.; Nakamura, N.; Inoue, K.; Koga, N.; Iwamura, H. *Chem. Eur. J.* **1996**, *2*, 259–264.
3. (a) Janssen, R. A. J.; Jansen, J. F. G. A.; van Haare, J. A. E. H.; Meijer, E. W. *Adv. Mater.* **1996**, *8*, 494–497; (b) Bosman, A. W.; Janssen, R. A. J.; Meijer, E. W. *Macromolecules* **1997**, *30*, 3606–3611.
4. Jansen, J. F. G. A.; Janssen, R. A. J.; de Brabander-van den Berg, E.-M. M.; Meijer, E. W. *Adv. Mater.* **1995**, *7*, 561–564.
5. Matyjaszewski, K.; Shigemoto, T.; Fréchet, J. M. J.; Leduc, M. *Macromolecules* **1996**, *29*, 4167–4171.
6. (a) Wayland, B. B.; Voorhees, S.-L.; Wilker, C. *Inorg. Chem.* **1986**, *25*, 4039–4042; (b) Wayland, B. B.; Poszmik, G. *Organometallics* **1992**, *11*, 3534–3542; (c) Mak, K. W.; Chan, K. S. *J. Am. Chem. Soc.* **1998**, *120*, 9686–9687.
7. (a) Ogoshi, H.; Setsune, J.; Omura, T.; Yoshida, Z. *J. Am. Chem. Soc.* **1975**, *97*, 6461–6466; (b) Wayland, B. B.; Sherry, A. E.; Poszmik, G.; Bunn, A. G. *J. Am. Chem. Soc.* **1992**, *114*, 1673–1681.
8. Hawker, C. J.; Fréchet, J. M. J. *J. Am. Chem. Soc.* **1990**, *112*, 7638–7647.
9. **1**-L1: UV–vis (CH_2Cl_2): 413.0, 523.0 nm; ^{1}H NMR (270 MHz, $CDCl_3$): δ 8.49 (s, 8H, pyrrole-β-H), 7.29 (s, 4H, *m*-H in $C_6H_2Me_3$), 7.23 (s, 4H, *m′*-H in $C_6H_2Me_3$), 5.42 (t, 1H, *p*-H in $C_6H_3(OMe)_2$), 3.02 (s, 6H, OMe), 2.62 (s, 12H, *p*-Me in $C_6H_2Me_3$), 2.55 (d, 2H, *o*-H in $C_6H_3(OMe)_2$), 2.00 (s, 12H, *o*-Me in $C_6H_2Me_3$), 1.72 (s, 12H, *o′*-Me in $C_6H_2Me_3$), −3.50 (d, 2H, Rh-C*H*$_2$-Ar); HRMS (FAB) calcd for $C_{65}H_{63}N_4O_2Rh$ (M^+): 1034.4006; found: 1034.4027. **1**-L3: UV–vis (CH_2Cl_2): 282.0, 413.0, 522.5 nm; ^{1}H NMR (270 MHz, $CDCl_3$): δ 8.49 (s, 8H, pyrrole-β-H), 7.32 (d, 8H, *o*, *m*-H in C_6H_4OMe), 7.22 (d, 8H, *m*-H in $C_6H_2Me_3$), 6.92 (d, 8H, *o*, *m*-H in C_6H_4OMe), 6.51 (t, 2H, *p*-H in 2nd layer Ar), 6.38 (d, 4H, *o*-H in 2nd layer Ar), 5.54 (t, 1H, *p*-H in 1st layer Ar), 4.93 (s, 8H, Ar-CH_2-OAr′ in 3rd layer Ar), 4.09 (s, 4H, Ar-CH_2-OAr′ in 2nd layer), 3.83 (s, 12H, outer OMe), 2.66 (d, 2H, *o*, -H in 1st layer Ar), 2.56 (s, 12H, *p*-Me in $C_6H_2Me_3$), 2.01 (s, 12H, *o*-Me in $C_6H_2Me_3$), 1.71 (s, 12H, *o′*-Me in $C_6H_2Me_3$), −3.51 (d, 2H, Rh-CH_2-Ar); MALDI-TOF-MS calcd for $C_{109}H_{103}N_4O_{10}Rh$ (M^+): 1730; found: 1730. **1**-L4: UV–vis (CH_2Cl_2): 281.0, 413.5, 523.0 nm; ^{1}H NMR (270 MHz, $CDCl_3$): δ 8.53 (s, 8H, pyrrole-β-H), 7.35 (d, 16H, *o*, *m*-H in C_6H_4OMe), 7.22 (d, 8H, *m*-H in $C_6H_2Me_3$), 6.90 (d, 16H, *o*, *m*-H in C_6H_4OMe), 6.67 (d, 8H, *o*-H in 3rd layer Ar), 6.58 (t, 4H, *p*-H in 3rd layer Ar), 6.53 (t, 2H, *p*-H in 2nd layer Ar), 6.41 (d, 4H, *o*-H in 2nd layer Ar), 5.59 (t, 1H, *p*-H in 1st layer Ar), 4.95 (s, 24H, Ar-CH_2-OMe), 2.70 (d, 2H, *o*-H in 1st layer Ar), 2.56 (s, 12H, *p*-Me in $C_6H_2Me_3$), 2.03 (s, 12H, *o*-Me in OAr′ in 3rd and 4th layers), 4.13 (s, 4H, Ar-CH_2-OAr′ in 2nd layer), 3.81 (s, 24H, outer $C_6H_2Me_3$), 1.72 (s, 12H, *o′*-Me in $C_6H_2Me_3$), −3.48 (d, 2H, Rh-CH_2-Ar); MALDI-TOF-MS calcd for $C_{169}H_{159}N_4O_{22}Rh$ (M^+): 2699; found: 2700. **1**-L5: UV–vis (CH_2Cl_2): 276.5, 413.5, 522.5 nm; ^{1}H NMR (270 MHz, $CDCl_3$): δ 8.49 (s, 8H, pyrrole-β-H), 7.30 (d, 32H, *o*, *m*-H in $C_6H_4OMe_3$), 7.17 (d, 8H, *m*-H in $C_6H_2Me_3$), 6.85 (d, 32H, *o*, *m*-H in $C_6H_4OMe_3$), 6.63 (m, 24H, *o*-H and *p*-H in 4th layer Ar), 6.51 (m, 14H, *p*-H in 2nd layer Ar, *o*-, *p*-H in 3rd layer Ar), 6.52 (t, 4H, *o*-H in 2nd layer Ar), 5.56 (t, 1H, *p*-H in 1st layer Ar), 4.89 (s, 56H, Ar-CH_2-OAr′ in 3rd, 4th, and 5th layers), 4.09 (s, 4H, Ar-CH_2-OAr′ in 2nd layer), 3.76 (s, 48H, outer OMe), 2.66 (d, 2H, *o*-H in 1st layer Ar), 2.50 (s, 12H, *p*-Me in $C_6H_2Me_3$), 1.99 (s, 12H, *o*-Me in $C_6H_2Me_3$), 1.68 (s, 12H, *o′*-Me in $C_6H_sMe_3$), −3.53 (d, 2H, Rh-CH_2-Ar); MALDI-TOF-MS calcd for $C_{289}H_{271}N_4O_{46}Rh$ (MH^+): 4636; found: 4637.
10. (a) Grigg, R.; Trocha-Grimshaw, J.; Viswanatha, V. *Tetrahedron Lett.* **1976**, *4*, 289–292; (b) Abeysekera, A. M.; Grigg, R.; Trocha-Grimshaw, J.; Viswanatha, V. *J. Chem. Soc., Perkin Trans. 1* **1977**, 36–44.